Supplementary Materials for

Anion-induced robust ferroelectricity in sulfurized pseudo-rhombohedral epitaxial $BiFeO_3$ thin films via polarization rotation

Guoqiang Xi[1], Zhao Pan[2*], Yue-Wen Fang[3,4*], Jie Tu[1], Hangren Li[1], Qianqian Yang[1], Chen Liu[5], Huajie Luo[6], Jiaqi Ding[7], Shuai Xu[2], Shiqing Deng[6], Qingxiao Wang[8], Dongxing Zheng[5], Youwen Long[2,9], Kuijuan Jin[2], Xixiang Zhang[5], Jianjun Tian[1], Linxing Zhang[1*]

[1]Institute for Advanced Materials Technology, University of Science and Technology Beijing, Beijing 100083, China

[2]Beijing National Laboratory for Condensed Matter Physics, Institute of Physics, Chinese Academy of Sciences, Beijing 100190, China

[3]Centro de Física de Materiales (CSIC-UPV/EHU), Manuel de Lardizabal pasealekua 5, 20018 Donostia/San Sebastián, Spain

[4]Fisika Aplikatua Saila, Gipuzkoako Ingeniaritza Eskola, University of the Basque Country (UPV/EHU), Europa Plaza 1, 20018 Donostia/San Sebastián, Spain

[5]Physical Science and Engineering Division, King Abdullah University of Science and Technology (KAUST), Thuwal 23955–6900, Saudi Arabia

[6]Beijing Advanced Innovation Center for Materials Genome Engineering, Department of Physical Chemistry, University of Science and Technology Beijing, Beijing 100083, China

[7]Key Laboratory for Micro/Nano Optoelectronic Devices of Ministry of Education, School of Physics and Electronics, Hunan University, Changsha 410082, China

[8]Corelab, King Abdullah University of Science and Technology (KAUST), Thuwal 23955–6900, Saudi Arabia

[9]Songshan Lake Materials Laboratory, Dongguan, Guangdong 523808, China

[*]Correspondence to: linxingzhang@ustb.edu.cn; zhaopan@iphy.ac.cn; fyuewen@gmail.com;

Methods

Thin-film synthesis. The epitaxial BFO thin films were grown on SRO layers deposited on single-crystalline (001) LAO substrates by using a radio frequency magnetron sputtering system (VJC-300, Beijing VNANO Vacuum Technology CO., LTD.). First, the SRO layers were deposited at their growth temperature of 680 ℃ under a mixed atmosphere of oxygen and argon (O:Ar=1:4); the sputtering pressure and power were 1.5 Pa and 50 W, respectively. Then, the epitaxial BFO thin films were grown on them at 500 ℃ under an O/Ar=3:1 atmosphere at 0.4 Pa, followed by annealing at 500℃ for 20 min. The anion substituted BFO thin films were prepared through a secondary treatment. A 0.2 M thiourea solution, dissolved in ethanol and water (solvent volume ratio of 4:1), was spin-coated onto the BFO thin films at 3000 rpm, followed by pyrolysis at 350 ℃ for 5 min and annealing for 20 min to obtain the BFOS thin films.

Structural and chemical characterization.

The θ-2θ scan of films were characterized by X-ray diffraction (XRD) with Cu Kα radiation. The structure and orientation of the thin films were investigated via synchrotron RSM measurements, which were conducted at the Diffuse X-ray Scattering Station of the Beijing Synchrotron Radiation Facility (BSRF), Beamline 1W1A. Besides, XAS measurements were performed at the photoelectron spectroscopy station of BSRF, Beamline 4B9B.

Electron microscopy analyses.

The STEM experiments were performed with a 200 kV JEOL ARM electron microscope equipped with double aberration correctors. To determine the B-site cation displacement vectors and domain structures, the noise in the HAADF–STEM images was reduced by HREM-Filters (HREM Research Inc.). The STEM–EDXS experiments were conducted at 200 kV with the Super EDS detectors. Accurate atomic positions in the STEM images were measured via the two-dimensional Gaussian fitting; all the polarization vector plots and *c/a* contour plots of the unit cells were obtained by using handmade scripts based on MATLAB.

Electrical measurements.

For macroscopic ferroelectric measurements, circular top Pt electrodes with a diameter of 50 μm and a thickness of ~ 20nm were deposited by magnetron sputtering. The ferroelectric hysteresis loops of the films were studied using TF-Analyzer 2000 (aixACCT).

SHG measurements.

The incident laser beam for the SHG measurements was generated by a Spectra Physics Maitai SP Ti:Sapphire oscillator whose central wavelength is 800 nm and repetition frequency is 82 MHz. The incident power was fixed at 50 mW and focused on the sample surface with a diameter of ~100 μm. The *p*-out and *s*-out configurations were adopted during measurement, which denote the arrangements where the analyzer polarization is parallel and vertical to the plane of incident light field, respectively. The polarization direction φ of the incident light field is adjusted by the rotation of the λ/2 waveplate driven by a rotating motor..

XPS and Raman spectroscopy measurements.

The XPS measurements were performed with a Thermo ESCALAB 250 spectrometer. Raman spectra of the thin films were measured by a Raman spectrometer (HR Evolution, Horiba, France) with a He–Cd excimer laser with a 325 nm wavelength in the backscattering geometry.

DFT calculations.

The first-principles DFT calculations were performed using the Vienna Ab initio Simulation Package (VASP).[1,2] The generalized gradient approximation in the form of the Perdew, Burke, and Ernzerhof exchange-correlation functional revised for solids (PBEsol)[3] was used with a Hubbard U correction in the Dudarev's form[4] for better treatment of Fe-3*d* electrons. The U value was set to 4 eV because it has been proven to be valid for the prediction of the rich variety of polymorphs of BFO[5] and doped BFO.[6] The plane wave energy cutoff was set to 400 eV. Unless otherwise noted, the models in this study use the experimental lattice parameters, and the internal coordinates were geometrically relaxed until the forces acting on each atom are less than 0.01 eV/Å and the difference in total energy between two consecutive electronic minimization steps was less than the 10^{-5} eV. The virtual crystal approximation (VCA)

is a method used to approximate the doped materials by treating the dopant atoms as "virtual" atoms that do not have a physical presence in the material. The VCA method is an efficient method for modeling doped materials and alloys with less computational cost than the method of using a number of large supercells, and was proven applicable for studying the atomic displacements and total energy for ferroelectric materials.[7]

Supplementary Information

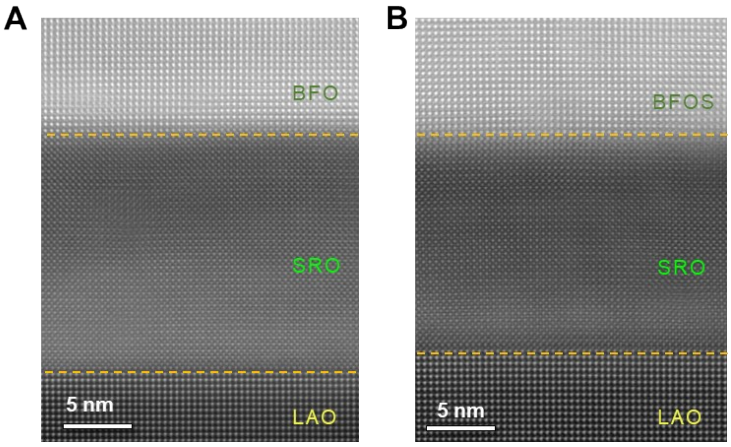

Fig. S1 HAADF–STEM images of the (**A**)BFO/SRO/LAO and (**B**)BFOS/SRO/LAO interfaces as viewed along the *a*-axis.

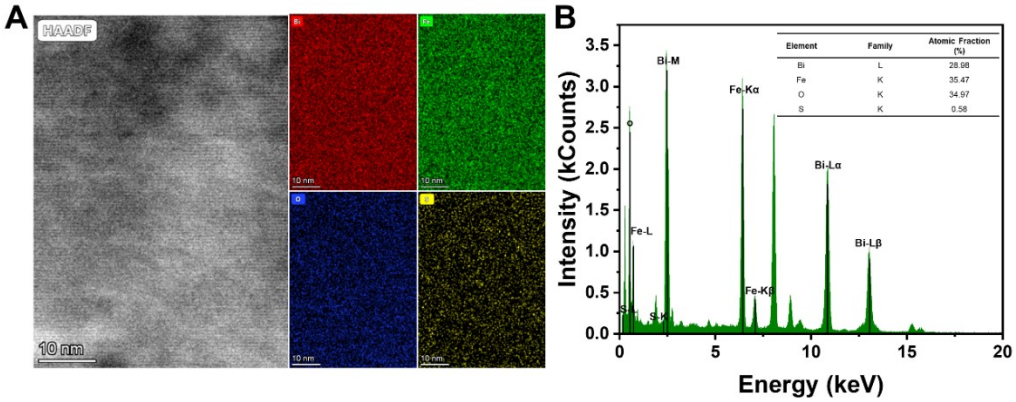

Fig. S2 (A) HADDF images and the corresponding energy-dispersive X-ray spectroscopy (EDX) elemental mapping of the BFOS film. **(B)** EDX spectra of the elements integrated from the corresponding elemental mapping results. The inset is the atomic fractions of bismuth, iron, oxygen, and sulfur.

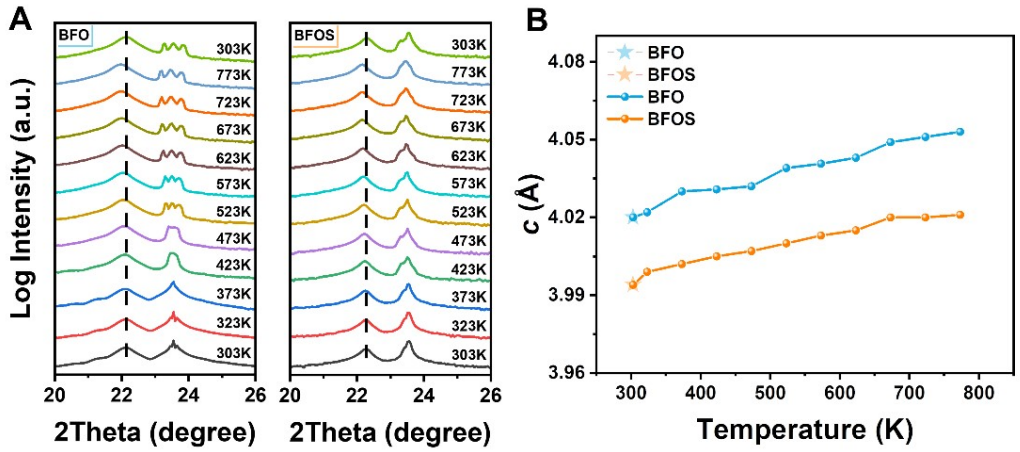

Fig. S3 (A) XRD pattern from room temperature to 773K. **(B)** The relationship between lattice constant *c* and temperature was obtained from diffraction peaks of (001) BFO and BFOS films. The results indicate that the out-of-plane lattice parameters BFO and BFOS films increase slightly with the temperature increase from room temperature to 773K. Subsequently, as the temperature decreases to room temperature, the films return to their initial state (star-shaped), exhibiting good thermal stability.

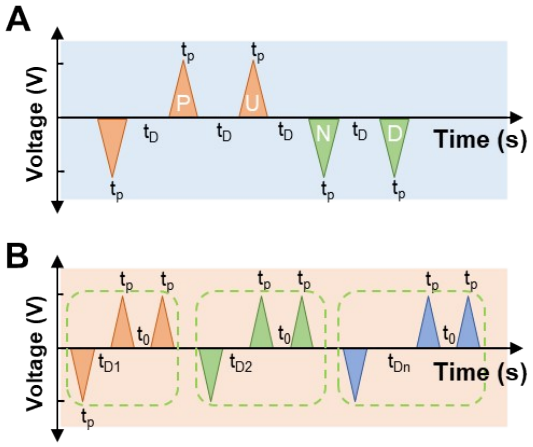

Fig. S4 (**A**) PUND measurement on films with 5 kHz electric field frequency for I–V and P–V loops. The first pulse is the prewrite pulse. After the preset pulse, the first read pulse is a positive switching pulse, the second is an unswitched pulse, the third is a negative switched pulse, and the last is a negative unswitched pulse. The pulse width (t_p) and the delay time between pulses (t_D) were 0.2 ms. (**B**) Modified PUND sequence used to measure the retention behavior of the samples; t_p was 0.5 ms and t_{D1}, t_{D2}, t_{Dn}, and t_0 are the delay times between pulses in the corresponding measurements where t_{D1}

and t_0 were 0.1 and 0.2 ms, respectively, while t_{Dn} varied.

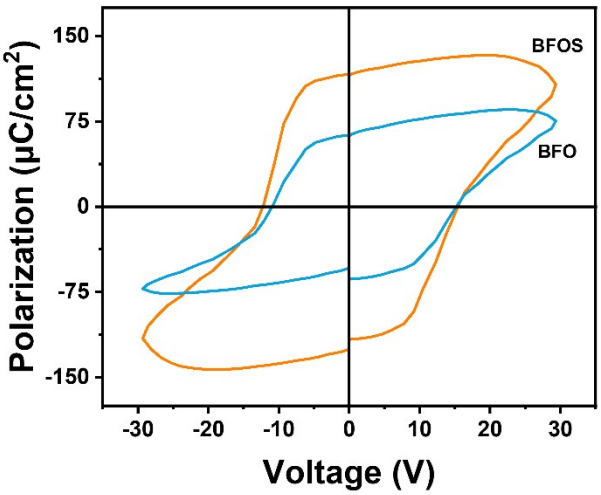

Fig. S5 The raw data ferroelectric hysteresis loops of BFO and BFOS films.

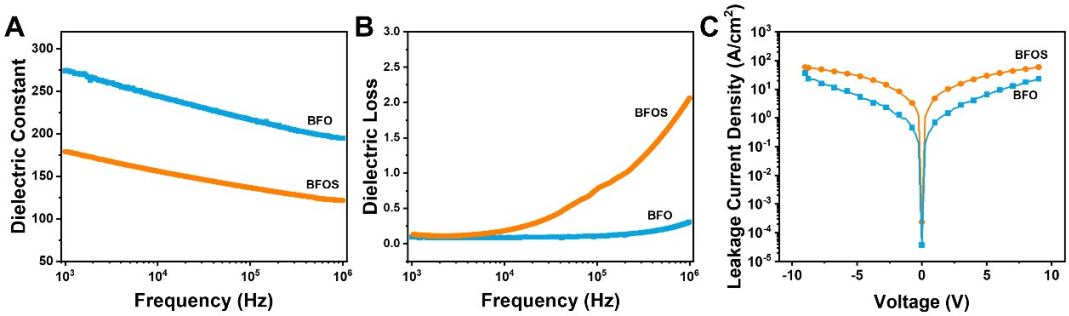

Fig. S6 (A) Dielectric constants and **(B)** loss tangents as a function of frequency for BFO and BFOS films. **(C)** Leakage current density via applied voltage curves for BFO and BFOS films at room temperature.

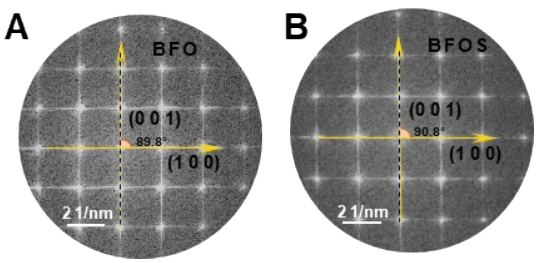

Fig. S7 Fast Fourier transform patterns along *a*-axis of the (**A**) BFO and (**B**) BFOS thin films.

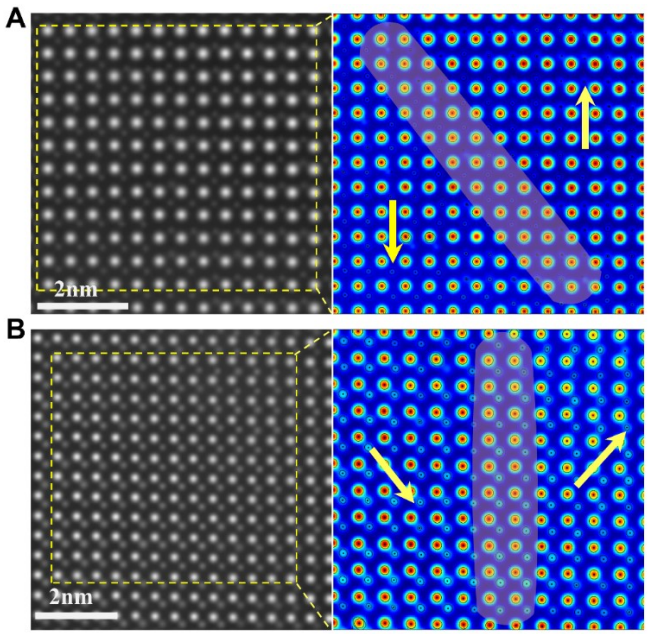

Fig. S8 HAADF–STEM images and atomic site fitting are shown for **(A)** BFO and **(B)** BFOS. The yellow arrows delineate the displacement of B-site cation relative to the lattice center of its four nearest neighboring A-site cations. The yellow area depicts the transition zone.

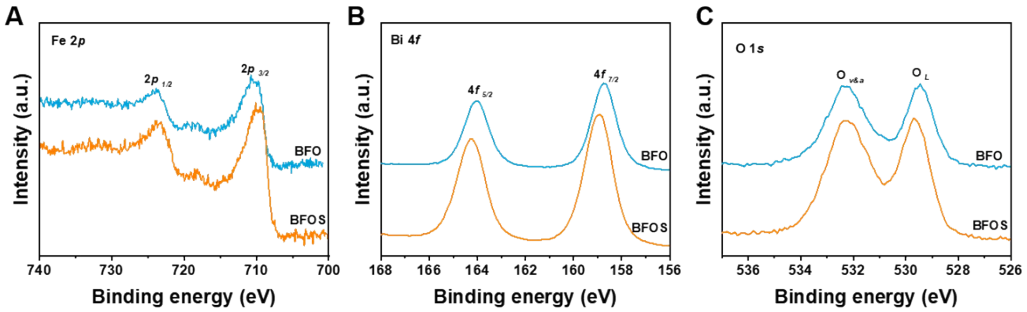

Fig. S9 X-ray photoelectron of (**A**) Fe 2*p*, (**B**) Bi 4*f*, and (**C**) O 1*s* spectra for BFO and BFOS thin films; the O_L and $O_{v\&a}$ indicate, respectively, the lattice oxygen and the sum of oxygen vacancies and absorbed oxygen atoms.

Reference

(1) Kresse, G. and Furthm¨uller, J., *Phys. Rev. B*, 1996, **54**, 11169.

(2) Kresse, G. and Furthm¨uller, J., *Comput. Mater. Sci.*, 1996, **6**, 15.

(3) Perdew, J. P., Ruzsinszky, A., Csonka, G. I., Vydrov, O. A., Scuseria, G. E., Constantin, L. A., Zhou, X., and Burke, K., *Phys. Rev. Lett.*, 2009, **102**, 039902.

(4) Dudarev, S. L., Botton, G. A., Savrasov, S. Y., Humphreys, C. J., and Sutton, A. P., *Phys. Rev. B*, 1998, **57**, 1505.

(5) Singh, A., Singh, V. N., Canadell, E., ´Iˇniguez, J., and Di´eguez, O., *Phys. Rev. Mater*. 2018, **2**, 104417.

(6) Fedorova, N. S., Nikonov, D. E., Li, H., Young, I. A., and ´Iˇniguez, J., *Phys. Rev. B*, 2022, **106**, 165122.

(7) Bellaiche, L., and Vanderbilt, D., *Phys. Rev. B*, 2000, **61**, 7877.